

# Scanning phase imaging without accurate positioning system

Tao Liu<sup>1</sup>, Bingyang Wang<sup>1</sup>, JiangTao Zhao<sup>2</sup>, Fu rong Chen<sup>3</sup> and Fucai Zhang<sup>1,\*</sup>

<sup>1</sup> Department of Electrical and Electronic Engineering, Southern University of Science and Technology, 1088 Xueyuan Avenue, Shenzhen 518055, China

<sup>2</sup> ESRF – The European Synchrotron, Grenoble, France

<sup>3</sup> Department of Materials Science and Engineering, City University of Hong Kong, Kowloon, China

\*Author to whom correspondence should be addressed: [zhangfc@sustech.edu.cn](mailto:zhangfc@sustech.edu.cn)

## ABSTRACT

Ptychography, a high-resolution phase imaging technique using precise in-plane translation information, has been widely applied in modern synchrotron radiation sources across the globe. A key requirement for successful ptychographic reconstruction is the precise knowledge of the scanning positions, which are typically obtained by a physical interferometric positioning system. Whereas high-throughput positioning poses a challenge in engineering, especially in nano or even smaller scale. In this work, we propose a novel scanning imaging framework that does not require any prior position information from the positioning system. Specifically, our scheme utilizes the wavefront modulation mechanism to reconstruct the object functions at each scan position and the shared illumination function, simultaneously. The scanning trajectory information is extracted by our subpixel image registration algorithm from the overlap region of reconstructed object functions. Then, a completed object function can be obtained by assembling each part of the reconstructed sample functions. High-quality imaging of biological sample and position recovery with sub-pixel accuracy are demonstrated in proof-of-concept experiment. Based on current results, we find it may have great potential applications in high-resolution and high throughput phase imaging.

## Introduction

Ptychography is a powerful phase imaging technique that can achieve nanoscale resolution beyond the probe size, by exploiting the redundant information from in-plane translation [1-5]. It has been developed for several decades and widely adopted in the synchrotron community [6-9]. However, conventional ptychography still relies on step scan mode to ensure accurate movement of scan positions, which overhead in data acquisition [10-12]. A faster alternative method, fly-scan mode been developed recently to deduce the overhead and accelerate the data acquisition procedure [13-16]. Whereas a

deblur algorithm must be used to eliminate the blurring effect introduced by continuous movement during exposure which in some cases reduce the image quality. Multi-beam ptychography, a fast alternative without blurring effect, has been proposed recently [17-19]. Such method increases the throughput of ptychography via several beams, but the image quality is less than satisfying. In all above ptychographic variations, accurate scanning position information is needed to guarantee a successful convergence, however, high accurate and throughput positioning system in nano or even small scale is challenging.

In this study, we investigate a novel imaging scheme achieving scanning phase imaging without any prior position information from the positioning system. We modify the conventional ptychography scheme by inserting a modulator downstream of the sample and uses the diffraction process to encode the information of both the modulator and the sample. This allows the reconstruction of the illuminated part of the sample with the corresponding diffraction pattern. The trajectory information can be extracted from the overlap region between each reconstructed sample functions. We validate the scheme in an optical experiment and show that it achieves high-quality reconstruction and subpixel accuracy in terms of the reconstructed position. We also discuss the physical and algorithmic modifications.

Proposed method has wide-ranging implications for research and engineering. Nanoprobe, for instance, a popular technique for high-resolution ptychographic imaging, relies on a highly stable and accurate motion system. Whereas, reducing the stage vibration down to a few or tens of nanometers is demanding and costly. Our method extracts position information from the proposed algorithm which frees ptychography from the positioning system. Furthermore, traditional ptychography uses a step-scan mode which is time-consuming. A faster alternative is fly-scan mode, but it usually degrades image quality and resolution, compared with the step scan mode. The single-shot imaging capability of our method would mitigate such degradation and benefit the in-situ ptychographic imaging.

## **Method**

The apparatus of proposed method for optical experiment is illustrated in the Fig.1. The beam filtered by a pinhole forms the probe. And the sample is partially illuminated by the probe in each scan, then, the exit wave gets modulated after free-space propagation for a period of distance  $Z_2$ . And the lens with focus  $Z_3$  is placed downstream of modulator to realize Fourier transform of the modulated exit wave. The diffraction intensity is, then, recorded by the detector placed in the focus plane of the lens.

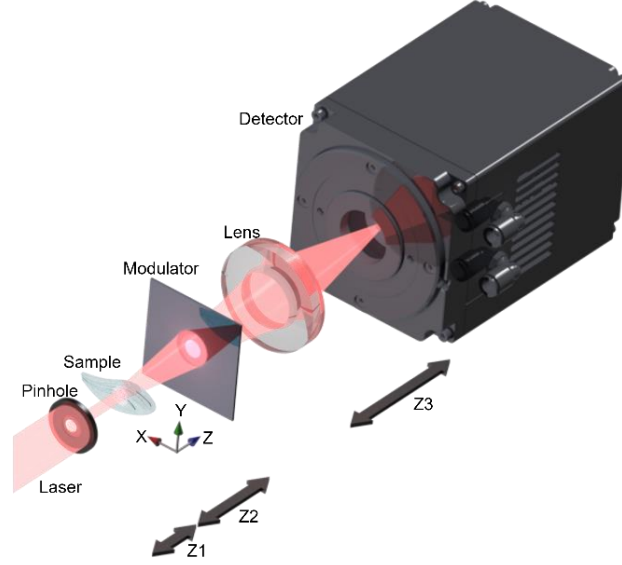


Fig. 1. Apparatus of proposed method. The probe is formed by a pinhole with finite diameter. And the sample is placed for a period of distance  $Z1$  from the pinhole. The modulator is placed downstream of the sample for distance  $Z2$ . And the lens between the modulator and the detector with focus  $Z3$  is used to perform Fourier transform.

The diffraction intensity datasets collected by the detector are used as input for the iterative reconstruction algorithm. The reconstruction procedure consists of two parts, as shown in Fig.2. Part 1 is the parallel reconstruction section, where we reconstruct the shared probe, the object functions corresponding to each diffraction pattern in parallel. In part 2, scan trajectory is extracted from the overlap region of object functions using our proposed image registration algorithm. After which, traditional ptychography engine is used to assemble the completed sample. The reconstruction steps are as follows:

- 1) Initialize the shared probe  $P(r)$ , object functions at each scan point  $O(r_j)$ , and compute the exit waves in the object plane.

$$\psi_o(r_j) = P(r) \times O(r_j). \quad (1)$$

Where  $r$  is the real space coordinate and  $r_j$  represent the translation position in real space which is measured in step11.

- 2) Propagate the exit waves from the sample plane to the front plane of the modulator.

$$\psi_{mf}(r_j) = P_1\{\psi_o(r_j)\}. \quad (2)$$

Here,  $P_1\{\cdot\}$  is the forward propagation operator from object to the modulator plane which, generally, angular-spectrum method is used.

- 3) Apply modulation to obtain the modulated exit waves in the rear plane of the modulator.

$$\psi_{mr}(r_j) = M(r) \times \psi_{mf}(r_j). \quad (3)$$

Where  $M(r)$  is the transmission function of the modulator.

- 4) Propagate the modulated exit waves to the detector plane.

$$\psi_a(q_j) = P_2\{\psi_{mr}(r_j)\}. \quad (4)$$

Where,  $P_2\{\cdot\}$  denotes the forward propagation operator between the modulator and the detector plane, Fourier transform is generally used. And  $q$  is the reciprocal space coordinate.

5) Apply the modulus constraint.

$$\hat{\psi}_a(q_j) = \frac{\psi_a(q_j)}{|\psi_a(q_j)|} \times \sqrt{I(q_j)}. \quad (5)$$

6) Propagate the revised modulated exit waves back to the rear plane of the modulator.

$$\hat{\psi}_{mr}(r_j) = P_2^{-1}\{\hat{\psi}_a(q_j)\}. \quad (6)$$

7) Undo modulation to obtain the revised exit waves in the front plane of the modulator.

$$\hat{\psi}_{mf}(r_j) = \psi_{mf}(r_j) + \frac{\alpha M^*(r) \times (\hat{\psi}_{mr}(r_j) - \psi_{mr}(r_j))}{\max(M(r) \times M^*(r))}. \quad (7)$$

In here,  $\alpha$  is the update coefficient, which is set as 0.9, generally.

8) Propagate the revised exit waves from the modulator front plane to the sample plane.

$$\hat{\psi}_o(r_j) = P_2^{-1}\{\hat{\psi}_{mf}(r_j)\}. \quad (8)$$

9) Update the shared probe and each part of the sample functions.

$$\hat{O}(r_j) = O(r_j) + \frac{\beta P^*(r) \times (\hat{\psi}_o(r_j) - \psi_o(r_j))}{\max(P(r) \times P^*(r))}. \quad (9)$$

$$\hat{P}(r) = P(r) + \frac{\beta \overline{O^*(r_j)} \times \overline{(\hat{\psi}_o(r_j) - \psi_o(r_j))}}{\max(\overline{O(r_j)} \times \overline{O^*(r_j)})}. \quad (10)$$

Where  $*$  denotes the complex conjugate and  $\beta$  is an update coefficient which usually is set as 0.9 ,  $\overline{\quad}$  denotes average operation.

10) Repeat steps 2-9 until the predetermined number of iterations is reached.

11) In proposed method, we assume that the scan trajectory is continuous, which means that adjacent scan points have an overlap region. Thus, the translation vector  $r_j$  can be searched, sequentially, with the proposed image registration operator  $Reg\{\cdot\}$ .

$$r_j = Reg\{O(r_{j-1}), O(r_j)\} \quad (11)$$

12) Employ a traditional ptychography engine  $Pty\{\cdot\}$  to refine the position and assemble the whole sample functions.

$$P(r), O(r) = Pty\{P(r), O(r_{1\dots j}), r_{1\dots j}\} \quad (12)$$

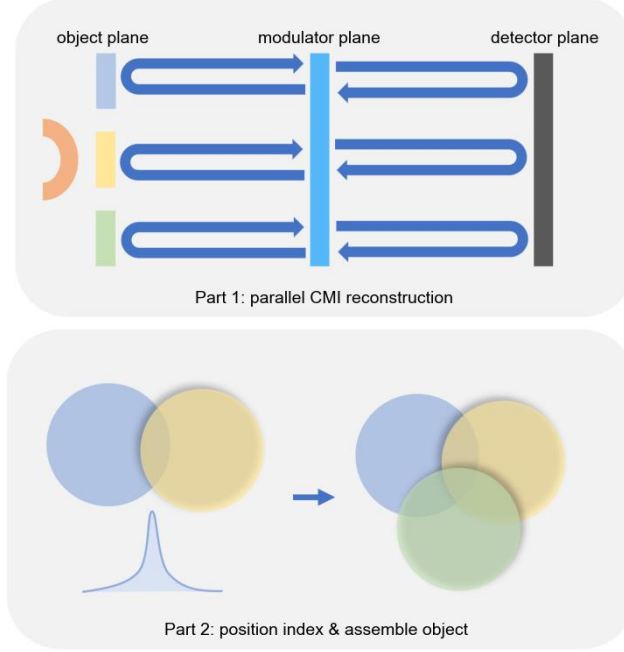


Fig. 2. Reconstruction procedure of proposed method. (a) Parallel CMI reconstruction section. (b) Position index and assembling section.

For the proposed method, scan trajectory is obtained by image registration algorithm rather than positioning system, thus, relative displacements between each part of sample should be calculated, precisely. In-plane translation of ptychography results gradient information in parallel with the relative displacement. Conventional gradient based image registration algorithms, generally, calculate the gradient along the X and Y axis which omits the gradient information along other directions. Herein, to exploit the gradient information of in-plane translation, we investigate a novel subpixel image registration algorithm named scaling gradient cross-correlation algorithm. Details of this algorithm are stated as follows:

Assume  $A, B$  are two  $M \times M$  images to be registered,  $K$  is the interpolation kernel,  $R$  is a mask of region of interest.

- 1) Apply the mask on these images.

$$A_R = A \times R, B_R = B \times R. \quad (13)$$

- 2) Interpolate images in the Fourier space using predefined interpolation kernel  $K$ .

$$A_I = \text{Int}\{\text{FFT}\{A_C\}, K\}, B_I = \text{Int}\{\text{FFT}\{B_C\}, K\}. \quad (14)$$

Here,  $\text{Int}\{\cdot\}$  is the interpolation operator,  $\text{FFT}\{\cdot\}$ .

- 3) Perform Inverse Fourier transform  $\text{IFFT}\{\cdot\}$  to get the scaled images.

$$A_S = \text{IFFT}\{A_I\}, B_S = \text{IFFT}\{B_I\}. \quad (15)$$

- 4) Calculate the scaling gradient of images.

$$G_A = A_S - A, G_B = B_S - B. \quad (16)$$

- 5) Calculate the cross-correlation spectrum  $CS$ .

$$CS = F\{G_A\} \times F\{G_B\}^*. \quad (17)$$

- 6) Calculate the displacement of these two images by indexing the peak.

$$\text{Ind}_{\{x\}}, \text{Ind}_{\{y\}} = \text{Index}\{CS\} \quad (18)$$

Here,  $\text{Ind}_{\{x\}}, \text{Ind}_{\{y\}}$  represents the displacement in  $x$  and  $y$  axis,  $\text{Index}\{\cdot\}$  is the indexing operator.

To validate the proposed method, we conduct an optical experiment with scheme shown in Fig.1. In our proof-of-concept experiment, the light source was a stabilized HeNe laser with a wavelength of  $632.8\text{ nm}$ . An aperture of  $0.85\text{ mm}$  diameter is used to shape the beam and placed it  $0.2\text{ mm}$  upstream of the sample. The sample was a fly wing. A continuous-type phase modulator with a scattering angle of  $5$  degrees was placed  $11.5\text{ mm}$  downstream of the sample. A Fourier lens with a focal length of  $30\text{ mm}$  was positioned between the modulator and the detector. The detector was a dhyanaV3 camera with a pixel size of  $6.5\text{ }\mu\text{m}$ .

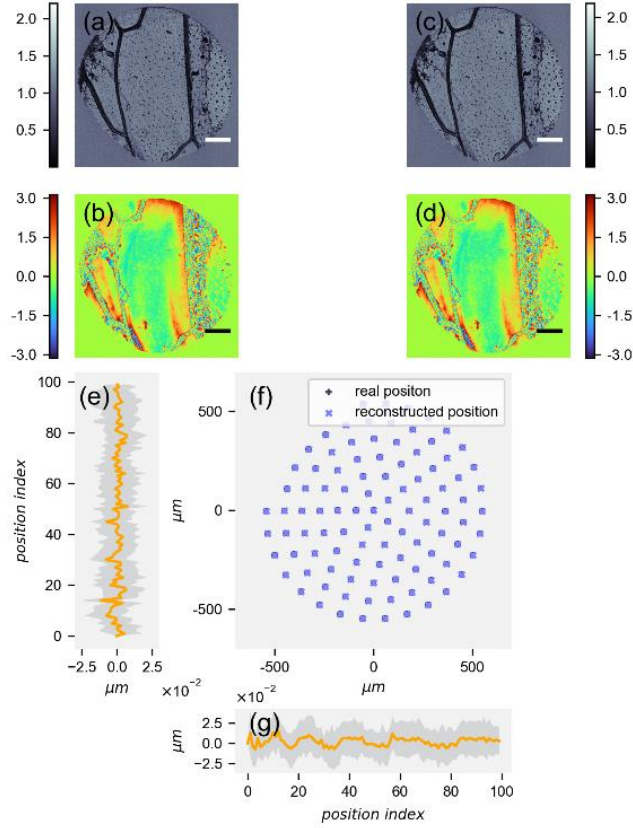


Fig. 3. Results of optical experiment. (a) and (b) Amplitude and phase of wing reconstructed with priori position information. (c) and (d) Amplitude and phase of wing reconstructed without priori position information. (e) and (g) Position error along the Y and X axis. The orange curve indicates the averaged position error of 100 reconstructions with different initial guess. Gray area represents the range of position error within 100 reconstructions. (f) Position plot of both real and reconstructed positions.

Figure 3 shows the results of an optical experiment in which the fly's wing is reconstructed with high quality. The amplitude and phase of the wing reconstructed with position information are shown in Figs.3(a) and 3(b), respectively. The amplitude and phase reconstructed without position information, shown in Figs.3(c) and 3(d), are in good agreement with those obtained with position information. Moreover, the reconstructed position in Fig.3(f) matches well with the actual one. The position errors along the Y and X axes are analyzed in Figs.3(e) and 3(g), respectively. In our scheme, the pixel size in the sample plane is  $2.9\text{ }\mu\text{m}$ . It is worth noting that the average position errors along both axes are less than  $0.01$  pixels, and the maximum position errors are also less than  $0.05$  pixels, which demonstrate the effectiveness and robustness of our proposed method.

## Discussion

One of the main innovations of our scheme is the insertion of a modulator downstream of the sample. The modulator is an optical component that remains fixed during the entire data acquisition process. The fixed modulator allows for single-shot imaging. However, in practice, the modulator may deviate from its ideal position due to various factors such as the variations of the holder. To study the robustness of our method against such effect, we randomly shifted the modulator in the reconstruction using the experimental data. The results of the reconstruction using a randomly shifted modulator are shown in Fig.4. The modulator at each scan point is shifted randomly within a range of 50 pixels, and the shifting vectors represented by orange arrow are shown in Fig.4(a). Since the sample and the modulator have a fixed relative position, the shift of the modulator induces a corresponding shift of the sample, as shown in Fig.4(b). The difference of amplitude reflects the shift of the sample, which is identical to that of the modulator. By algorithmically aligning all the shifted samples, our proposed method can still recover the scan trajectory and complete the reconstruction. The reconstructed amplitude and phase of the sample shown in Figs.4(c) and 4(d) are in good agreement with the original ones shown in Figs.3(a) and 3(b).

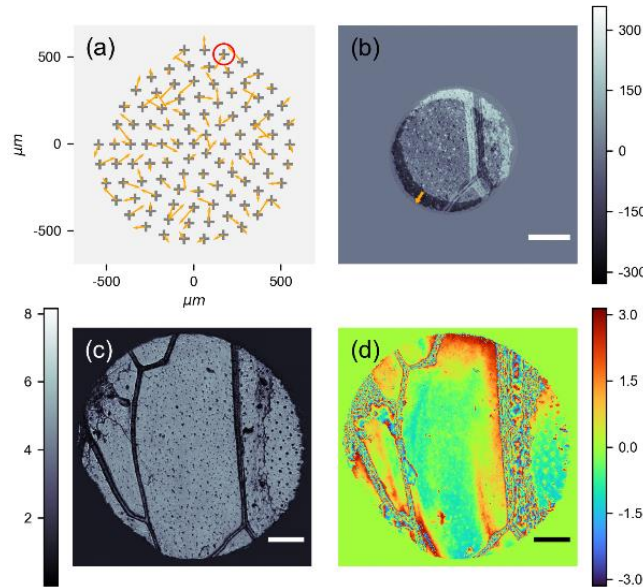


Fig. 4. Reconstructed sample with randomly shifted modulator. (a) The shift plot of modulator in which the gray cross marks represent the scan position. And the orange arrows are shifting vector of modulator. (b) The difference of reconstructed amplitude of sample with original and shifted modulator for the point marked by red circle in (a). (c) and (d) The amplitude and phase of reconstructed sample with randomly shifted modulator.

## Conclusion

In conclusion, this letter reports a novel scanning phase imaging method utilizing wavefront modulation concepts and subpixel image registration algorithm based on scaling gradient. Optical experiment for biological sample has been carried out to validate the proposed method. Both visual comparison of reconstructed sample and quantitative analysis of the position information have been presented. Hence, the position error ranges from 0.01-0.05 pixels over 100 reconstructions with different initial guess have demonstrated the effectiveness of our proposed method.

Despite the proof-of-concept experiment, we also conduct discussion about hardware and software modifications that we made to the traditional ptychography scheme. On the one hand, we discuss the deviation of modulator and

found that it has negligible effect on the reconstruction when the modulator is randomly shifted within 50 pixels. On the other hand, the proposed method obtains position information from our proposed new image registration algorithm, rather than traditional positioning system.

Our work may have important implications in research and engineering areas. For scientific research, the proposed method may benefit the high-resolution ptychographic imaging by providing accurate position information because high-precision positioning is demanding, especially when employing nano probe. What's more, the temporal resolution of ptychography can also be enhanced by the single-shot capability of our method which is paramount for in-situ study. For engineering aspect, our method releases the requirement of detector dynamic range by using a modulator to scatter the photons. Also, the expensive and complicated positioning system is significant for ptychography imaging. Proposed method obtains position information from algorithm can, therefore, reduce the dependence of positioning system.

### Conflict of Interest

Conflict of Interest The authors have no conflicts to disclose.

### Data availability

The data that support the findings of this study are available from the corresponding author upon reasonable request.

### References

1. Pfeiffer, F. X-ray ptychography. *Nature Photon* 12, 9–17 (2018). <https://doi.org/10.1038/s41566-017-0072-5>
2. Mille, N., Yuan, H., Vijayakumar, J. *et al.* Ptychography at the carbon K-edge. *Commun Mater* 3, 8 (2022). <https://doi.org/10.1038/s43246-022-00232-8>
3. Thibault, P. *et al.* High-resolution scanning X-ray diffraction microscopy. *Science* 321, 379–382 (2008).
4. Maiden, A. M. & Rodenburg, J. M. . An improved ptychographical phase retrieval algorithm for diffractive imaging. *Ultramicroscopy* 109, 1256–1262 (2009).
5. Chapman, H., Nugent, K. Coherent lensless X-ray imaging. *Nature Photon* 4, 833–839 (2010). <https://doi.org/10.1038/nphoton.2010.240>
6. Sakdinawat, A. & Attwood, D. Nanoscale X-ray imaging. *Nature Photon.* 4, 840–848 (2010).
7. Miao, J. *et al.* Extending the methodology of X-ray crystallography to allow imaging of micrometre-sized non-crystalline specimens. *Nature* 400, 342–344 (1999).
8. Nugent, K. A. Coherent methods in the X-ray sciences. *Adv. Phys.* 59, 1–99 (2010).
9. Holler, M. *et al.* An instrument for 3d x-ray nano-imaging. *Rev. Sci. Instrum.* 83, 073703 (2012).
10. Nazaretski, E. *et al.* Design and performance of a scanning ptychography microscope. *Rev. Sci. Instrum.* 85, 033707 (2014).
11. Dierolf, M. *et al.* Ptychographic x-ray computed tomography at the nanoscale. *Nature* 467, 436–440 (2010).
12. Holler, M. *et al.* X-ray ptychographic computed tomography at 16 nm isotropic 3d resolution. *Sci. Rep.* 4, 3857 (2014).
13. Huang, X., Lauer, K., Clark, J. *et al.* Fly-scan ptychography. *Sci Rep* 5, 9074 (2015). <https://doi.org/10.1038/srep09074>
14. McNulty, I. *et al.* Design and performance of the 2-id-b scanning x-ray microscope. *Proc. SPIE.* 3449, 67–74 (1998).
15. Kilcoyne, A. *et al.* Scanning x-ray microdiffraction with submicrometer white beam for strain/stress and orientation mapping in thin films. *J. Synchrotron Radiat.* 10, 125–136 (2003).
16. Thibault, P. & Menzel, A. Reconstructing state mixtures from diffraction measurements. *Nature* 494, 68–71 (2013).



17. Hirose, M., Higashino, T., Ishiguro, N. & Takahashi, Y. Multibeam ptychography with synchrotron hard X-rays. *Opt. Express* 28, 1216 (2020).
18. Yao, Y., Jiang, Y., Klug, J.A. *et al.* Multi-beam X-ray ptychography for high-throughput coherent diffraction imaging. *Sci Rep* 10, 19550 (2020). <https://doi.org/10.1038/s41598-020-76412-8>
19. Bevis, C. *et al.* Multiple beam ptychography for large field-of-view, high throughput, quantitative phase contrast imaging. *Ultramicroscopy* 184, Part A, 164–171 <https://doi.org/10.1016/j.ultramic.2017.08.018>.(2017).